# Differential contribution of the three Aph1 genes to γ-secretase activity *in vivo*

**Lutgarde Serneels*, Tim Dejaegere*, Katleen Craessaerts*, Katrien Horré*, Ellen Jorissen*, Thomas Tousseyn*, Sébastien Hébert*, Marcel Coolen†, Gerard Martens†, An Zwijsen‡, Wim Annaert§, Dieter Hartmann*, and Bart De Strooper*¶**

*Neuronal Cell Biology and §Membrane Transport Laboratories, and ‡Department of Developmental Biology, Flanders Interuniversity Institute for Biotechnology and Katholieke Universiteit Leuven, Leuven B-3000, Belgium; and †Department of Molecular Animal Physiology, Radboud University Nijmegen, 6500 Nijmegen, The Netherlands

Edited by Kai Simons, Max Planck Institute of Molecular Cell Biology and Genetics, Dresden, Germany, and approved December 18, 2004 (received for review December 1, 2004)

**γ-Secretase is the protease responsible for amyloid β peptide release and is needed for Notch, N-Cadherin, and possibly other signaling pathways. The protease complex consists of at least four subunits, i.e., Presenilin, Aph1, Pen2, and Nicastrin. Two different genes encode Aph1A and Aph1B in man. A duplication of *Aph1B* in rodents has given rise to a third gene, *Aph1C*. Different mixes of γ-secretase subunits assemble in at least four human and six rodent complexes but it is not known whether they have different activities *in vivo*. We report here the inactivation of the three *Aph1* genes in mice. *Aph1A*$^{-/-}$ embryos show a lethal phenotype characterized by angiogenesis defects in the yolk sac, neuronal tube malformations, and mild somitogenesis defects. *Aph1B*$^{-/-}$ or *C*$^{-/-}$ or the combined *Aph1BC*$^{-/-}$ mice (which can be considered as a model for total *Aph1B* loss in human) survive into adulthood. However, *Aph1BC*$^{-/-}$ deficiency causes a mild but significant reduction in amyloid β percursor protein processing in selective regions of the adult brain. We conclude that the biochemical and physiological repercussions of genetically reducing γ-secretase activity via the different *Aph1* components are quite divergent and tissue specific. Our work provides *in vivo* evidence for the concept that different γ-secretase complexes may exert different biological functions. In the context of Alzheimer's disease therapy, this implies the theoretical possibility that targeting specific γ-secretase subunit combinations could yield less toxic drugs than the currently available general inhibitors of γ-secretase activity.**

Alzheimer | intramembrane cleavage | Presenilin | knockout

The multimolecular complex γ-secretase cleaves proteins in their transmembrane domain. The complex consists of at least four subunits called Presenilin (Psen), Nicastrin (Nct), Pen2, and Aph1 (1–3). The Psens provide the catalytic subunits of the complex (4), although the precise functional contribution of the other subunits remains to be clarified. Mutations in the genes encoding presenilin 1 (PSEN1) or its homologue presenilin 2 (PSEN2) cause familial Alzheimer's disease (5, 6). Besides amyloid β (Aβ) precursor protein (APP), γ-secretase cleaves an increasing list of type I transmembrane proteins including Notch (7) and N-Cadherin (8) (for a full review, see ref. 9).

Until now, γ-secretase has largely been considered as a homogenous activity, but especially in mammals the situation is probably more complicated (10). Two different *Psen* genes and two (human) or three (rodent) *Aph1* genes that can be alternatively spliced have been identified. Aph1A or Aph1B and Psen1 or Psen2 are incorporated in a mutually exclusive way into different complexes as demonstrated recently, providing formal proof that at least four different complexes in man (and six in mouse) can be generated (11, 12). The question remains however whether those different complexes have also different physiological functions. Because γ-secretase is considered a potential drug target in Alzheimer's disease, a better understanding of the heterogeneity of this enzymatic activity is also of considerable medical importance. In this regard, Aph1 is highly interesting because, like Psen, it is a variable component of the γ-secretase complex. Loss of function of the single genes in *Caenorhabditis elegans* (13, 14), and *Drosophila melanogaster* (15) causes Notch signaling deficiencies. It is not known, however, to what extent the three Aph1 genes contribute to γ-secretase signaling in *Mus musculus* and to what extent they are involved in APP processing in the brain. Here, we address this question by a genetic approach, inactivating the three known *Aph1* genes in mice.

## Materials and Methods

For more detailed information, see *Supporting Text*, which is published as supporting information on the PNAS web site.

**Generation of Aph1 Knockout Mice.** Conditionally targeted (*Aph1A* and *-C*) or classically targeted (*Aph1B*) mice were generated as detailed in *Supporting Text*. Animals carrying a null allele were obtained after breeding with transgenic mice expressing a *Pgk* driven Cre-recombinase. Determinations of the genotypes of the floxed or knockout mice or yolk sac of embryos were done by Southern blotting or PCR analysis.

**Histology.** Mice and embryos beyond embryonic day 14 (E14) were perfused via the left ventricle with either 6% glutaraldehyde or Bouin's solution diluted 1:4 in PBS or with 10% neutral buffered formaline. Younger embryos (E8.5–E13.5) were fixed by immersion. Serial sections (7 μm) were cut, and the central sections of each series were stained with hematoxylin and eosin for standard light microscopy. Adjacent sections were used for immunohistological screening. A tyramide-based signal amplification technique (NEN-Dupont) was applied. For transmission and scanning EM, embryos were fixed in 6% glutaraldehyde and 2% $OsO_4$. Postfixed embryos were dehydrated and then embedded in Araldite. For scanning EM, postfixed specimens were dehydrated, equilibrated with 100% acetone, and dried in a Polaron CPD 7501 critical point dryer by using liquid carbon dioxide. After mounting, gold coating ("sputtering") was done with an Agar automatic coater.

**Embryonic Fibroblast Culture and Recombinant Adenovirus Infection.** Mouse embryonic fibroblast (MEF) cultures were derived from dissociated *Aph1*-deficient mouse embryos and littermate controls (16, 17). Subconfluent MEF cell lines were infected with recombinant adenovirus with a multiplicity of infection of 500

This paper was submitted directly (Track II) to the PNAS office.

Abbreviations: Aβ, amyloid β; APP, Aβ precursor protein; E*n*, embryonic day *n*; MEF, mouse embryonic fibroblast; CTF, C-terminal fragment.

¶To whom correspondence should be addressed. E-mail: bart.destrooper@med.kuleuven.ac.be.

(18). Control infections were done with recombinant adenovirus bearing GFP cDNA.

**Luciferase Reporter Assays for γ-Cleavage.** γ-Secretase cleavage of APP or Notch was determined as the ratio between the luciferase activities of the γ-secretase-dependent variant (APPΔC99-Gal4-VP16, NotchΔE-Gal4-VP16) and the mean luciferase activities of the γ-secretase-independent signal obtained with Gal4-VP16.

## Results

**Targeted Inactivation of the Three Mouse *Aph1* Genes.** *Aph1* deficient (Aph1$^{-/-}$) mice were generated by homologous recombination (Fig. 6, which is published as supporting information on the PNAS web site). The *Aph1A* gene was targeted conditionally with loxP sequences in intron 2 and intron 8 (Aph1$A^{flx}$). Subsequent Cre-mediated excision of the region between the loxP sites generated an *Aph1A* null allele (*Aph1A*$^{-}$ see Fig. 6*A*). To inactivate *Aph1B*, an alkaline phosphatase reporter sequence was inserted in frame in exon 1. A neomycin resistance gene was inserted in intron 2. This *Aph1B* construct was electroporated into wild-type ES cells and in the ES cell line with one *Aph1C* allele already conditionally targeted (Fig. 6*B*). The latter was necessary to obtain *Aph1BC* double-targeted ES clones because the two genes are genetically closely linked. Inserting loxP sites into intron 2 and intron 4 (*Aph1C*$^{flx}$) conditionally inactivated the *Aph1C* gene. Recombination results in the deletion of exons 3 and 4 and a frame shift in the ORF of the rest of the *Aph1C* gene (deletion from amino acid 96 on). Homozygous floxed *Aph1A*$^{flx/flx}$ and *Aph1C*$^{flx/flx}$ mice were viable and fertile. Reverse transcriptase experiments on total RNA derived from the MEF's or brains of the *Aph1A*$^{flx/flx}$ and *Aph1C*$^{flx/flx}$ mice demonstrated that the Aph1 mRNA was expressed from the floxed Aph1 alleles but not from the null alleles (*Aph1A*$^{-/-}$ and *Aph1C*$^{-/-}$) obtained after Cre-recombinase (data not shown).

**Destabilization of the γ-Secretase Components in the Absence of *Aph1A*.** Successful targeting of the three genes was confirmed at the DNA and the mRNA level by using Southern and RT-PCR experiments (Fig. 7, which is published as supporting information on the PNAS web site). We also confirmed the knockout of the different *Aph* genes by Western blotting of fibroblasts derived from knockout animals (Fig. 1). Aph1A is absent from *Aph1A*$^{-/-}$ cells and staining with Aph1BC antibodies demonstrated that no major compensatory up-regulation of Aph1B and -1C protein occurs. (Fig. 1*A*, the antibodies do not discriminate between the highly similar Aph1B and Aph1C protein). Similarly, no significant compensatory up-regulation of Aph1A is observed in the Aph1B$^{-/-}$, the Aph1C$^{-/-}$, or the double Aph1BC$^{-/-}$ fibroblast cell lines (Fig. 1*B*). When Aph1C$^{-/-}$-protein extracts were probed with the Aph1BC antibodies, a reduced signal is observed, reflecting the residual presence of Aph1B protein. In the *Aph1B*$^{-/-}$ cell line, a (weak) residual Aph1C staining is also observed after longer exposure of the blot (Fig. 1*B Inset*). Accordingly, in the *Aph1BC*$^{-/-}$ double-deficient cell line, no specific staining is seen with Aph1BC antibodies. We conclude that all three *Aph1* genes are expressed at the protein level in embryonic fibroblasts and that a full knockout of each of the three genes is obtained.

We analyzed membrane fractions from the different cell lines for the expression of the different γ-secretase components. Only deficiency of Aph1A had a significant effect on Nct glycosylation and Nct, Pen2, and Psen expression levels (Fig. 1*C*), whereas Aph1B, Aph1C, or Aph1BC deficiency had little or no effects on the other γ-secretase complex proteins (Fig. 8, which is published as supporting information on the PNAS web site). The latter probably reflects the relative low expression of the Aph1BC proteins in these cells, because overexpression of transfected Aph1C in *Aph1A*$^{-/-}$ cells restored complex formation (results not shown).

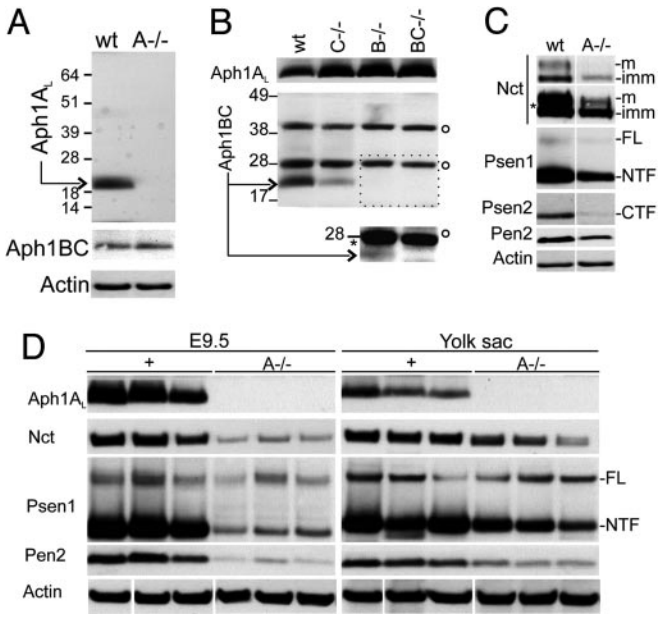


**Fig. 1.** Knockout of Aph1A, but not Aph1B, and Aph1C affects γ-secretase complex. (*A*) Western blot analysis of cell extracts from wild-type (wt) and homozygous (A−/−) *Aph1A* $^{-/-}$ MEFs using antibodies against Aph1A$^{L}$, Aph1BC, and actin. Staining with Aph1BC antibodies demonstrated no major compensatory up-regulation of Aph1B and -1C protein. (*B*) Western blot analysis of cell extracts from wild-type (wt) and homozygous single Aph1C$^{-/-}$, Aph1B$^{-/-}$ and double Aph1BC$^{-/-}$ MEFs using antibodies against Aph1A$^{L}$ and Aph1BC. After longer exposure, a reduced signal (asterisk) is observed in the *Aph1B*$^{-/-}$ cells. *Aph1BC*$^{-/-}$ double-deficient cell line showed no specific staining with the Aph1BC antibodies. The open circle denotes unspecific signals. (*C*) Western blot analysis of cell extracts from wild-type (wt) and homozygous (A−/−) *Aph1A* $^{-/-}$ MEFs using antibodies raised to Nct, Psen1 (NTF), Psen2 (CTF), Pen2, and Actin. Nct glycosylation maturation is disturbed, but not completed abolished (asterisk indicates overexposed panel). Psen-cleaved fragments are reduced, whereas Psen holoprotein (FL) levels are unchanged. Pen2 protein is severely reduced in *Aph1A*$^{-/-}$. (*D*) Western blot analysis of extracts from wild-type or heterozygous (+) and *Aph1A*$^{-/-}$(A−/−) embryos proper and their yolk sacs using the indicated antibodies.

We extended our biochemical analysis also to tissues *in vivo*, confirming deficient γ-secretase complex assembly in yolk sac and embryo proper (Fig. 1*D*).

***Aph1A*-Deficient Mice Are Embryonic Lethal.** No obvious abnormalities were observed in heterozygous *Aph1A*$^{+/-}$ mice. Viable homozygous *Aph1A*$^{-/-}$ mice (as defined by beating heart) were

**Table 1. Progenies of crosses of *Aph1* heterozygous mice**

| | | | Genotype, *n* | | |
|---|---|---|---|---|---|
| | Age | Total, *n* | +/+ | +/− | −/− |
| | E8.5 | 43 | 13 | 20 | 10 |
| | E9.5 | 74 | 22 | 33 | 19 |
| *Aph-1A* | E10.5 | 36 | 9 | 20 | 4 (5) |
| | E11.5 | 10 | 4 | 6 | 0 |
| | 3 weeks | 166 | 63 | 103 | 0 |
| *Aph-1B* | 3 weeks | 67 | 21 | 32 | 14 |
| *Aph-1C* | 3 weeks | 248 | 75 | 109 | 64 |
| *Aph-1BC* | 3 weeks | 84 | 17 | 51 | 16 |

The value in parentheses indicates five additional *Aph1A*$^{-/-}$ embryos that were recovered but probably dead (as defined by no beating heart).

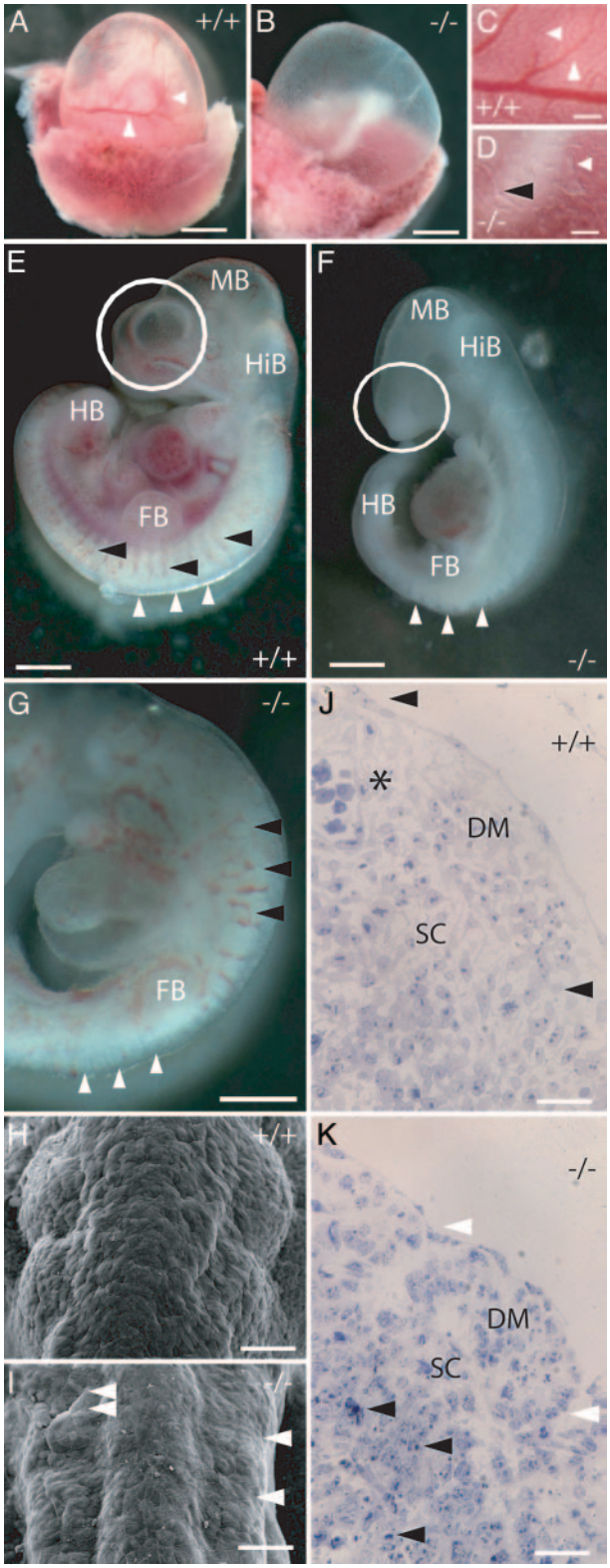


**Fig. 2.** Severely impaired vascular development but only mild somitogenesis defects in *Aph-1A*$^{-/-}$ mice. (*A–D*) Yolk sac vascular reorganization is defective in Aph-1A-deficient mice. Normal reorganization of vascular primordia between E8.5 and E9.5 in wild-type embryos establishes a hierarchically organized vascular tree (arrows in *A* and *C*). This tree is completely absent in Aph-1A$^{-/-}$ mice (*B* and *D*). Only isolated blood forming islands (white arrow in *D*) and short Y-shaped vascular profiles (black arrowhead in *D*) are visible. (*E–G*) *Aph-1A*$^{-/-}$ embryos (*F* and *G*) at E10.5 develop a body axis that extends well beyond the hindlimb bud (HB) but remains thin caudal to the fore limb bud (FB). Note that intersomitic blood vessels develop, but display irregular patterning (black arrowheads in *E* and *G*). Somite development in *Aph-1A*$^{-/-}$ extends along the entire body axis (white arrows in *E–G*) up to the level of the hindlimb bud anlage. Note the hypoplastic development of forebrain hemispheres (white circles). (*H–K*) Somites (shown at the level of the hindlimb bud in *H* and *I*) remain smaller than normal and form only shallow bulges beneath the ectoderm, sometimes appearing even collapsed (double white arrow head in *I*). Intersomitic sulci are likewise less prominent, but are present bilaterally in a fairly symmetric fashion (white arrowheads). Numerous apoptotic cells are evidenced by their condensed nuclei (black arrowheads in K). Note that intersomitic blood vessels are readily seen in wild type embryos (asterisk). (Scale bars, 400 $\mu$m in *A* and *B*, 50 $\mu$m in *C* and *D*, 300 $\mu$m in *E–G*, 50 $\mu$m in *H* and *I*, and 30 $\mu$m in *J* and *K*.) HB, hindlimb bud; FB, forelimb bud; HiB, hindbrain; MB, midbrain; DM, dermatomyotome; SC, sclerotome.

found up to E10.5, but never thereafter (Table 1). From E9.5 onwards, *Aph1A*$^{-/-}$ mice are smaller and moderately shorter than their wild-type littermates (Fig. 2*F*). Compared to mice with a complete loss of γ-secretase activity (*Psen1&2*$^{-/-}$ or *Nct*$^{-/-}$), the caudal body axis at E10.5 extends significantly further, and regular hind limb buds and a short stretch of the tail anlage are observed.

**Angiogenesis.** The *Aph1A*$^{-/-}$ mice fail to develop an organized vascular system in their yolk sacs. At E10.5, only isolated blood-forming islands or short Y-shaped vascular fragments were observed (Fig. 2 *A–D*). Calibre irregularities and patterning defects are also seen in the intersomitic aortic branches (Fig. 2 *G* and *K*). Heart looping occurs in the correct orientation (Fig. 2*G*), but is inconstantly accompanied by a distended pericardial sac as in *Psen* double-deficient mice (data not shown).

**Somitogenesis.** Aph1A$^{-/-}$ embryos display normal embryonic turning (Fig. 2*F*). In contrast to *Psen1*/*Psen2*$^{-/-}$ or *Nct*$^{-/-}$ mice, in which somite formation is characteristically abrogated after the fourth to fifth rostral somite pair (i.e., at the forelimb bud level), somite segmentation in *Aph1A*$^{-/-}$ mice goes on up to at least the hind limb buds (Fig. 2 *G* and *I*). Although the bilateral symmetric segmentation appears to be intact, the somites are smaller than normal and feature a shallow, less regular external contour bulging beneath the surface ectoderm (Fig. 2*I*). The latter correlates with a less well organized dermatomyotome and a high proportion of apoptotic cells in the sclerotome (Fig. 2*K*).

**Neural Tube.** From E8.5, on neural tube "kinking" is observed (Fig. 3*B*). From E9.5 onwards, the growth of the telencephalon anlage is visibly retarded, evidenced by either absent or hypoplastic hemispheric vesicles (Fig. 2*F*). The strictly radial orientation of neuroepithelial cells in the neural tube is severely disturbed (Fig. 3 *D* and *E*), and numerous cells emigrate into the surrounding mesoderm (Fig. 3*D*). In addition, cells with pyknotic nuclei or extensive surface blebbing, both indicative of apoptosis, are encountered in the neuroepithelium (Fig. 3*E*) and the surrounding mesoderm (Fig. 3*G*). Apoptotic cell death was confirmed by immunostaining for cleaved caspase 3 (Fig. 3*I*). It should be noticed that also large areas existed in the neuronal tube and mesoderm in which no overt signs of cell death could be identified.

Taken together, the loss of *Aph1A* leads to a mosaic phenotype that combines traits of a full loss of γ-secretase deficiency (yolk sac) with that of a partial deficit (somitogenesis). Additional *in situ* hybridization experiments on embryos confirmed the strong expression of *Aph1A* in yolk sac and embryo proper which largely overlapped with the expression of the other γ-secretase components *Psen1*, *Pen2*, and *Nct* (Fig. 9, which is published as supporting information on the PNAS web site).

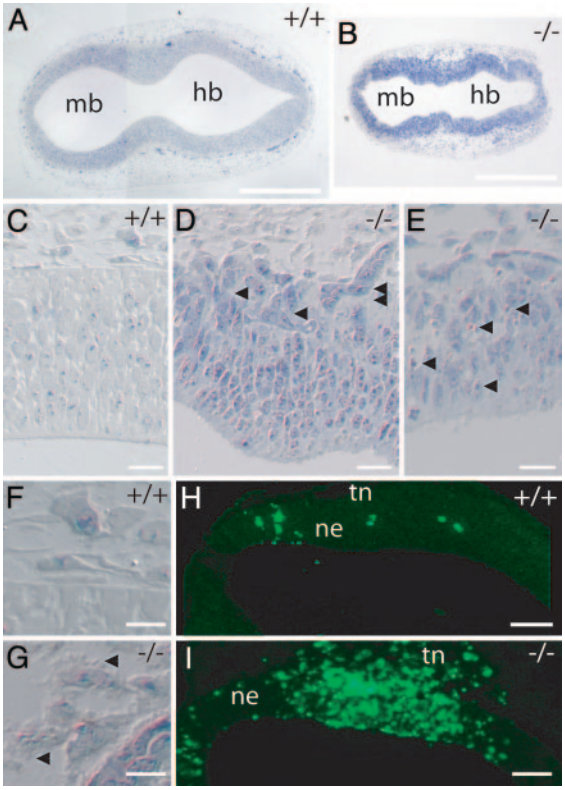


**Fig. 3.** *Aph-1A*$^{-/-}$ affects neural tube formation. (*A* and *B*) *Aph-1A*$^{-/-}$ embryos display a highly irregular contour of the neural tube. (*C–E*) The strict radial organization of neural tube epithelia between lumen and head mesenchyme is partially lost in knockout mice. Within the neural tube, numerous cells are aligned obliquely (single arrowheads in *D*). Notice the multifocal emigration of neural cells into the surrounding mesenchyme (double arrowheads in *D*). Individual or grouped apoptotic cells are observed within the neural tube (arrows in *E*) and especially in the surrounding mesoderm (note massive surface blebbing indicated with arrowheads in *G*). Apoptosis is confirmed by immunostaining of cleaved caspase 3 (*H* and *I*) and also affects the trigeminal neural crest underlying the nasal and otic placodes and the head mesenchyme (tn in *H* and *I*). (Scale bars, 200 $\mu$m in *A* and *B*, 30 $\mu$m in *C–E*, 20 $\mu$m in *F* and *G*, and 100 $\mu$m in *H* and *I*). mb, midbrain; hb, hindbrain, ne, neuroepithelium; tn, trigeminal neural crest cells.

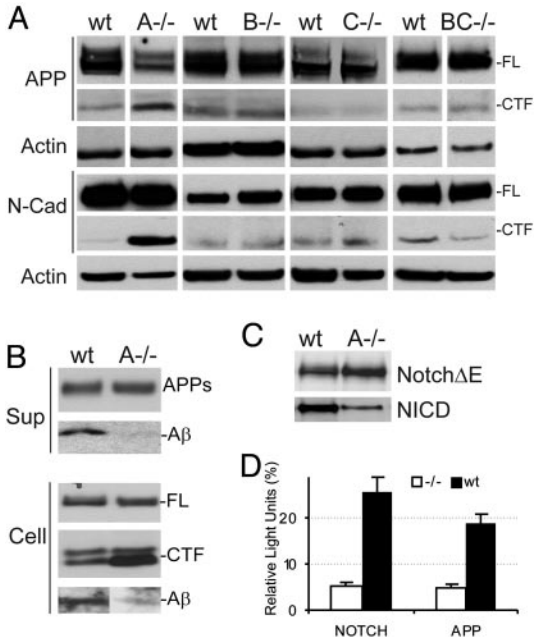


**Fig. 4.** Single *Aph1A* deficiency causes decreased γ-secretase activity. (*A*) Western blot analysis of cell extracts from wild-type (wt) and *Aph1*$^{-/-}$ (*A*−/−, *B*−/−, *C*−/−, and *BC*−/−) MEFs using antibodies against the C terminus of APP, N-Cadherin, and Actin. Note the accumulation of endogenous APP-CTF and N-Cadherin CTF in the absence of Aph1A. (*B*) Wild-type (wt) and *Aph1A*$^{-/-}$ (A−/−) MEFs were infected with recombinant adenovirus expressing APPsw or GFP. Aβ, APPs, and full-length APP (FL) and APP CTFs are indicated. Intracellular Aβ was immunoprecipitated and stained with mAb WO-2. (*C*) Wild-type (wt) and *Aph1A*$^{-/-}$ (A−/−) MEFs were infected with recombinant adenovirus expressing NotchΔE (myc tagged) or GFP and cell extracts were analyzed by Western blot using antibodies raised against the cleaved Notch (Val-1744) receptor and the myc epitope. (*D*) Wild-type and *Aph1A*$^{-/-}$ fibroblasts were transfected with APPΔC99-Gal4-VP16, NotchΔE-Gal4-VP16, or Gal4-V16 and UAS-luciferase. The luciferase activities of the γ-secretase-dependent variants (APPΔC99-Gal4-VP16, NotchΔE-Gal4-VP16) were normalized for the luciferase activities obtained with the γ-secretase-independent Gal4-VP16. Values are presented as means of three assays ± SEM.

**Normal Overall Phenotype of *Aph1B*- and *Aph1C*-Deficient Mice.** The *Aph1B*$^{-/-}$, *Aph1C*$^{-/-}$, and *Aph1BC*$^{-/-}$ homozygous mice were viable and fertile, and offspring derived from heterozygous crosses were born in normal Mendelian ratios (Table 1). Preliminar microscopical inspection of tissues that express relatively high levels of Aph1B and Aph1C like brain, kidney, and testis (11) did not reveal any significant aberrations (results not shown).

**APP and Notch Processing Are Equally Affected by the Absence of *Aph1A*.** We next analyzed the effect of the different *Aph1* deficiencies on γ-secretase activity in the embryonic fibroblasts by evaluating the levels of endogenous APP and N-cadherin (N-Cad) C-terminal fragments (CTF). These fragments are the direct substrates for γ-secretase and they accumulate when this activity is decreased. In agreement with the embryonic phenotype, only in *Aph1A*$^{-/-}$ fibroblasts could accumulation of APP-CTF and N-Cad-CTF be demonstrated (Fig. 4*A*). It should be noticed that a decreased expression of full-length APP is observed as well, which could indicate a regulatory loop between APP-CTF accumulation (or inhibition of APP intracellular domain generation) and APP steady state levels of expression (19). An important question is whether any of the Aph1 components differentially contribute to the cleavage of APP or Notch. Therefore, we transduced fibroblasts with human APP or with a NotchΔE construct and measured directly the generation of Aβ peptide or NICD (Fig. 4 *B* and *C*). Aph1A deficiency dramatically inhibited both APP and Notch processing. Although Aβ generation seemed to be more strongly affected than NICD release (Fig. 4*B*, row indicated with Aβ, and 4*C*, row indicated with NICD), these assays rely on different antibodies, making it difficult to compare them directly. Therefore, we transfected fibroblasts with a UAS-luciferase reporter gene and an APP or a Notch reporter construct that include a Gal4-VP16 sequence in their cytoplasmic domains. In this experiment, the only variable is the transmembrane domain, and readout can therefore directly be compared for the two substrates. In this assay (Fig. 4*D*), both APP and Notch processing are affected to a similar extent by Aph1A deficiency (≈70% inhibition).

**Alterations in APP Processing in *Aph1BC*$^{-/-}$ Adult Brain.** From our previous work, we know that Aph1BC is expressed relatively more abundantly in brain (11). Therefore, we analyzed the repercussions of *Aph1BC*$^{-/-}$ deficiency in different regions of adult brain on expression of the other γ-secretase subunits and APP processing (as reflected by changes in APP-CTF levels; Fig. 5).

The absence of Aph1BC affected Psen1 and Pen2 steady state levels (most clearly seen in the brainstem extracts). Aph1A

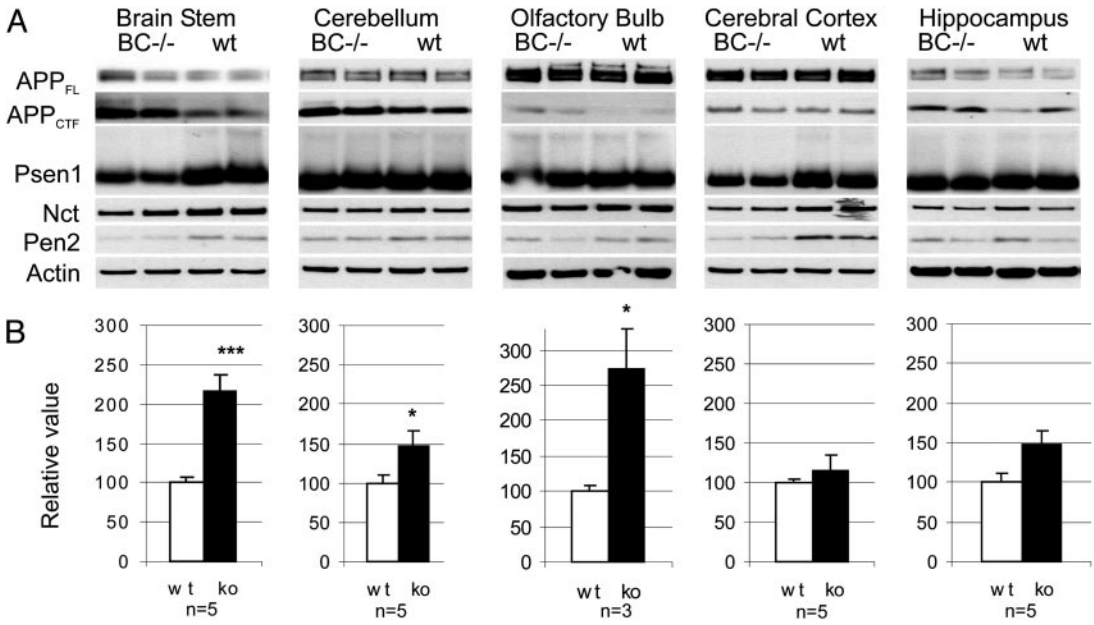


**Fig. 5.** Aph1BC deficiency causes decreased γ-secretase activity in selective brain regions. (*A*) Western blot analysis of brain extracts from wild-type (wt) and *Aph1BC*$^{-/-}$ littermate mice using antibodies against APP (CTF), Psen-1 (NTF), Nct, Pen-2, and actin as a loading control. (*B*) Quantification of the relative accumulation of APP-CTFs. The densitometric values obtained for APP-CTF in *Aph1BC*$^{-/-}$ brain regions were normalized to the average signal for APP-CTF in the corresponding wild-type region (=100%). Statistically significant differences are indicated by asterisks (*, $P < 0.05$; ***, $P < 0.001$). The number of independent mice analyzed per brain region is indicated at the bottom of each graph.

expression was not significantly changed (not shown), indicating no compensatory up-regulation of this component. More importantly, in brainstem and olfactory bulb, a strong, >2-fold accumulation of APP-CTF was observed. In other brain regions, a small accumulation of APP-CTF was observed that reached only statistical significance in the cerebellum.

## Discussion

The three rodent *Aph1* genes were successfully targeted by homologous recombination as demonstrated by Southern blotting and RT-PCR analysis of the different mouse lines obtained. The absence of protein expression was confirmed by Western blotting. The *Aph1A*$^{-/-}$ mice display an embryonic lethal phenotype, whereas the *Aph1B*$^{-/-}$ and *Aph1C*$^{-/-}$ mice display a normal phenotype with no gross abnormalities in fertility, survival, or anatomy. In that regard, they are even less affected than the *Psen2*$^{-/-}$ mice, which have also a quite normal overall phenotype, but suffer from lung hemorrhages and fibrosis in adulthood (20–22). It should be noted that *Aph1B* and *Aph1C* are highly similar (96.3% at the nucleotide level) and that both genes are clustered on chromosome 9. Most likely, they arose by rodent-specific gene duplication (11, 23). Because both genes are actively transcribed (shown here), we targeted the two genes consecutively on the same chromosome. The *AphBC*$^{-/-}$ was also compatible with survival into adulthood and further breeding. However, at the biochemical level, the *Aph1BC*$^{-/-}$ mice displayed a very interesting phenotype, showing accumulation of APP-CTF in specific regions of the adult mouse brain. Such an accumulation of APP-CTF indicates deficient γ-secretase processing, as has been demonstrated in various Psen- and Nct-deficient mice and cell lines (21, 24, 25).

A question that needs to be addressed here is whether the quite spectacular "loss of *Aph1A* function" phenotype can entirely be explained by an impaired γ-secretase activity. The vascular reorganization deficits in the yolk sac have been observed in the severe loss of function of γ-secretase seen in *Psen1&2*$^{-/-}$ mice (20, 21) and *Nct*$^{-/-}$ mice (24). Two other major features of the *Aph1A*$^{-/-}$ phenotype (apoptosis and neuroepithelial emigration from the neural tube) have previously not been recognized but are also aspects of severe γ-secretase deficiency, as we observed when reinvestigating our *Psen1&2*$^{-/-}$ mice (T.T. and D.H., unpublished observations). In contrast, somite segmentation, which is severely affected in *Psen1&2*$^{-/-}$ mice, appears to be relatively preserved in the *Aph1A*$^{-/-}$ mice. Because a severe defect of body axis extension and mesoderm segmentation is also seen in *Nct*$^{-/-}$ mice (24), it is reasonable to conclude that the relative mild effects of the *Aph1A* deficiency on somitogenesis reflect a residual level of γ-secretase activity in this tissue that is sufficient to maintain at least partially the Notch-driven segmentation clock (26). It should be noted that the somites of a Notch-1 processing deficient mouse that was generated by mutating the γ-secretase (S3) cleavage site were also only moderately affected (27), suggesting that relatively low levels of (cleavage dependent) Notch signaling are sufficient to maintain this developmental process. The conclusion that *Aph1A* deficiency reflects essentially impaired γ-secretase function is further confirmed by *in situ* hybridization experiments demonstrating the overlap in expression of Aph1A and other γ-secretase components (Fig. 9), and the biochemical analysis demonstrating the decreased expression of the other γ-secretase components in *Aph1A*$^{-/-}$ yolk sac and embryo proper (Fig. 1*D*). However, we cannot completely rule out the theoretical possibility that *Aph1A* exerts also more subtle non-γ-secretase functions that remain to be discovered.

The loss of γ-secretase component expression in *Aph1A*$^{-/-}$ fibroblasts apparently causes an ≈70% reduction in γ-secretase activity (Fig. 4*D*). This decrease roughly corresponds to the activity of a single *Psen1* knockout, whereas the phenotypical alterations are more similar to the severe phenotype observed in *Psen1&2*$^{-/-}$ embryos that are 100% deficient in γ-secretase processing. It has to be left open for the moment whether these differences in the *Aph1A* and *Psen1* null phenotypes are due to subtle differences in the activity of Psen1 deficient versus Aph1A-deficient γ-secretase complexes *in vivo* that were not

readily seen in the fibroblast cell culture analysis. Alternatively, subtle differences in tissue expression of the different isoforms of the γ-secretase complex, with, for example, Aph1A complexes playing a key role in vasculogenesis, could explain the observed heterogeneity in function of the different γ-secretase complexes.

A third important point are the specific deficiencies in γ-secretase processing of APP observed in the brain of *Aph1BC*-deficient mice. These results are in line with recent findings in a rat model for neurodevelopmental disorders (23). In these rats, a genetic recombination event in the Aph1B and -C locus resulted in diminished Aph1BC expression and changes in γ-secretase cleavage activity in brain regions in a pattern quite similar to our observations in mice. These rats display several neurobehavioral abnormalities, like increased sensitivity to apomorphine, changes in prepulse and latent inhibition, and others (23) that segregate with the different levels of Aph1BC expression. Thus, from an Alzheimer's disease therapy point of perspective, the survival of *Aph1BC*-deficient mice into adulthood suggests that the Aph1BC-containing complexes might be a less problematic drug target than the Aph1A containing complexes, although the rat studies indicate that the repercussions have to be further evaluated at the psychopharmacological level. This situation is not very different from the BACE-1 target (28). The Aph1A subgroup of γ-secretase complexes in contrast has a central role in development, and is likely also involved in the main γ-secretase functions in adulthood.

We thank Christian Haass (Ludwig-Maximilian-University, Munich) for Aph1BC serum 435G and Rafi Kopan (Washington University, St. Louis) for the NotchΔE construct. This research was supported by a Pioneer award from the Alzheimer's Association (to B.D.S.); the Fund for Scientific Research, Flanders (Belgium); the Katholieke Universiteit Leuven (Geconcerteerde Onderzoeksactie); the European Union (Abnormal Proteins in the Pathogenesis of Neurodegenerative Disorders); and the Federal Office for Scientific Affairs, Belgium (Inter-University Network for Fundamental Research P5/19). T.D. is an aspirant of the Fund for Scientific Research.

1. Edbauer, D., Winkler, E., Regula, J. T., Pesold, B., Steiner, H. & Haass, C. (2003) *Nat. Cell Biol.* **5,** 486–488.
2. Takasugi, N., Tomita, T., Hayashi, I., Tsuruoka, M., Niimura, M., Takahashi, Y., Thinakaran, G. & Iwatsubo, T. (2003) *Nature* **422,** 438–441.
3. Kimberly, W. T., LaVoie, M. J., Ostaszewski, B. L., Ye, W., Wolfe, M. S. & Selkoe, D. J. (2003) *Proc. Natl. Acad. Sci. USA* **100,** 6382–6387.
4. Wolfe, M. S., Xia, W., Ostaszewski, B. L., Diehl, T. S., Kimberly, W. T. & Selkoe, D. J. (1999) *Nature* **398,** 513–517.
5. Hardy, J. & Selkoe, D. J. (2002) *Science* **297,** 353–356.
6. Annaert, W. & De Strooper, B. (2002) *Annu. Rev. Cell Dev. Biol.* **18,** 25–51.
7. De Strooper, B., Annaert, W., Cupers, P., Saftig, P., Craessaerts, K., Mumm, J. S., Schroeter, E. H., Schrijvers, V., Wolfe, M. S., Ray, W. J., *et al.* (1999) *Nature* **398,** 518–522.
8. Marambaud, P., Shioi, J., Serban, G., Georgakopoulos, A., Sarner, S., Nagy, V., Baki, L., Wen, P., Efthimiopoulos, S., Shao, Z., *et al.* (2002) *EMBO J.* **21,** 1948–1956.
9. Kopan, R. & Ilagan, M. X. (2004) *Nat. Rev. Mol. Cell. Biol.* **5,** 499–504.
10. De Strooper, B. (2003) *Neuron* **38,** 9–12.
11. Hébert, S. S., Serneels, L., Dejaegere, T., Horré, K., Dabrowski, M., Baert, V., Annaert, W., Hartmann, D. & De Strooper, B. (2004) *Neurobiol. Dis.* **17,** 260–272.
12. Shirotani, K., Edbauer, D., Prokop, S., Haass, C. & Steiner, H. (2004) *J. Biol. Chem.* **279,** 41340–41345.
13. Goutte, C., Tsunozaki, M., Hale, V. A. & Priess, J. R. (2002) *Proc. Natl. Acad. Sci. USA* **99,** 775–779.
14. Francis, R., McGrath, G., Zhang, J., Ruddy, D. A., Sym, M., Apfeld, J., Nicoll, M., Maxwell, M., Hai, B., Ellis, M. C., *et al.* (2002) *Dev. Cell* **3,** 85–97.
15. Hu, Y. & Fortini, M. E. (2003) *J. Cell Biol.* **161,** 685–690.
16. Herreman, A., Van Gassen, G., Bentahir, M., Nyabi, O., Craessaerts, K., Mueller, U., Annaert, W. & De Strooper, B. (2003) *J. Cell Sci.* **116,** 1127–1136.
17. Hartmann, D., De Strooper, B., Serneels, L., Craessaerts, K., Herreman, A., Annaert, W., Umans, L., Lubke, T., Lena Illert, A., von Figura, K. & Saftig, P. (2002) *Hum. Mol. Genet.* **11,** 2615–2624.
18. Nyabi, O., Bentahir, M., Horre, K., Herreman, A., Gottardi-Littell, N., Van Broeckhoven, C., Merchiers, P., Spittaels, K., Annaert, W. & De Strooper, B. (2003) *J. Biol. Chem.* **278,** 43430–43436.
19. von Rotz, R. C., Kohli, B. M., Bosset, J., Meier, M., Suzuki, T., Nitsch, R. M. & Konietzko, U. (2004) *J. Cell Sci.* **117,** 4435–4448.
20. Donoviel, D. B., Hadjantonakis, A. K., Ikeda, M., Zheng, H., Hyslop, P. S. & Bernstein, A. (1999) *Genes Dev.* **13,** 2801–2810.
21. Herreman, A., Hartmann, D., Annaert, W., Saftig, P., Craessaerts, K., Serneels, L., Umans, L., Schrijvers, V., Checler, F., Vanderstichele, H., *et al.* (1999) *Proc. Natl. Acad. Sci. USA* **96,** 11872–11877.
22. Steiner, H., Duff, K., Capell, A., Romig, H., Grim, M. G., Lincoln, S., Hardy, J., Yu, X., Picciano, M., Fechteler, K., *et al.* (1999) *J. Biol. Chem.* **274,** 28669–28673.
23. Coolen, M. W., Van Loo, K. M. J., Van Bakel, N. N. H. M., Pulford, D. J., Serneels, L., De Strooper, B., Ellenbroek, B. A., Cools, A. R. & Martens, G. J. M. (2005) *Neuron*, in press.
24. Li, T., Ma, G., Cai, H., Price, D. L. & Wong, P. C. (2003) *J. Neurosci.* **23,** 3272–3277.
25. Yu, H., Saura, C. A., Choi, S. Y., Sun, L. D., Yang, X., Handler, M., Kawarabayashi, T., Younkin, L., Fedeles, B., Wilson, M. A., *et al.* (2001) *Neuron* **31,** 713–726.
26. Aulehla, A. & Herrmann, B. G. (2004) *Genes Dev.* **18,** 2060–2067.
27. Huppert, S. S., Le, A., Schroeter, E. H., Mumm, J. S., Saxena, M. T., Milner, L. A. & Kopan, R. (2000) *Nature* **405,** 966–970.
28. Harrison, S. M., Harper, A. J., Hawkins, J., Duddy, G., Grau, E., Pugh, P. L., Winter, P. H., Shilliam, C. S., Hughes, Z. A., Dawson, L. A., *et al.* (2003) *Mol. Cell Neurosci.* **24,** 646–655.